

Correlations and Semi-Universal Relations Connecting Nuclear Matter and Neutron Stars

J. M. Lattimer

Department of Physics & Astronomy



STONY BROOK UNIVERSITY



U.S. DEPARTMENT OF
ENERGY

Office of Science



Many-Particle Systems Under Extreme Conditions
Polish-German WE-Aeraeus Seminar & Max Born Symposium

Görlitz, Germany, Dec. 3–6, 2023

Acknowledgements

Funding Support:

DOE - Nuclear Physics

DOE - Toward Exascale Astrophysics of Mergers and Supernovae (TEAMS)

NASA - Neutron Star Interior Composition ExploreR (NICER)

NSF - Neutrinos, Nuclear Astrophysics and Symmetries (PFC - N3AS)

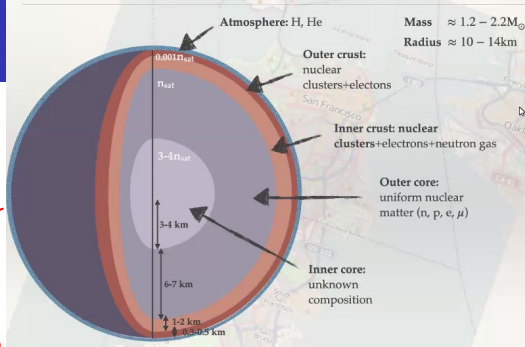
DOE - Nuclear Physics from Multi-Messenger Mergers (NP3M)

Recent Collaborators:

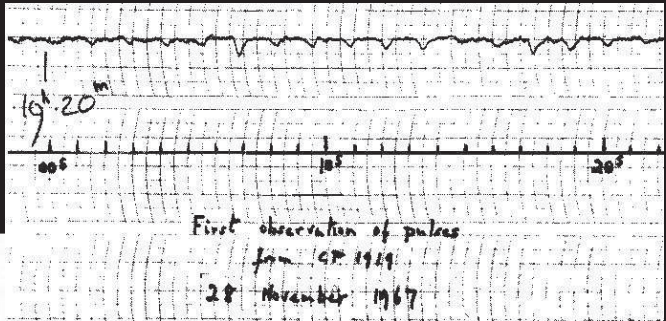
Boyang Sun (Stony Brook), Duncan Brown & Soumi De (Syracuse), Christian Drischler, Madappa Prakash & Tianqi Zhao (Ohio), Sophia Han (TDLI), Sanjay Reddy (INT), Achim Schwenk (Darmstadt), Andrew Steiner (Tennessee) & Ingo Tews (LANL)

Neutron Stars: Basics

- Nearly all known NSs are pulsars (rapidly rotating and highly magnetized) that emit X-ray, optical or radio beams from their poles, like a lighthouse.
- The radii of most NSs are about 12 km.
- Most, if not all, NSs are formed in the gravitational collapse of massive stars at the ends of their lives; some of those collapses produce black holes instead. Some massive NSs may be formed in the aftermath of a binary merger of two lower-massed neutron stars.
- The minimum possible NS mass is $0.1M_{\odot}$, but none are observed to be less massive than $1M_{\odot}$.



The Discovery of Pulsars



PhD student **Jocelyn Bell** and
Prof. **Antony Hewish**
Initially “**Little Green Men**”
Hewish won Nobel Prize in 1974

Crab Nebula SN1054AD



Proves that some supernovae produce p
Anasazi Indian cave pictogram,
Chaco Canyon, NM

O

**Pulsar rotates
30 times
per second!**

Pulsars are Precise Clocks

PSR J0437-4715

At 00:00 UT Jan 18 2011:

$$P = 5.7574519420243 \text{ ms} \\ \pm 0.0000000000001 \text{ ms}$$


The last digit changes by 1 every half hour!

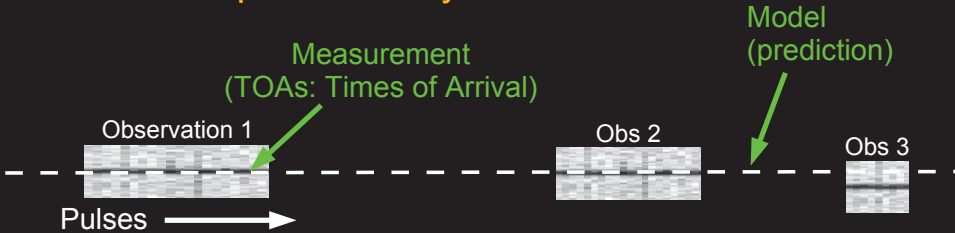
This digit changes by 1 every 500 years!

This extreme precision is what allows us to
use pulsars as tools to do unique physics!

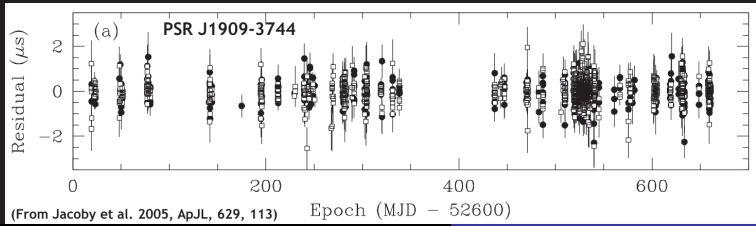
Pulsar Timing:

Pulse Phase Tracking

Unambiguously account for every rotation of a pulsar over years



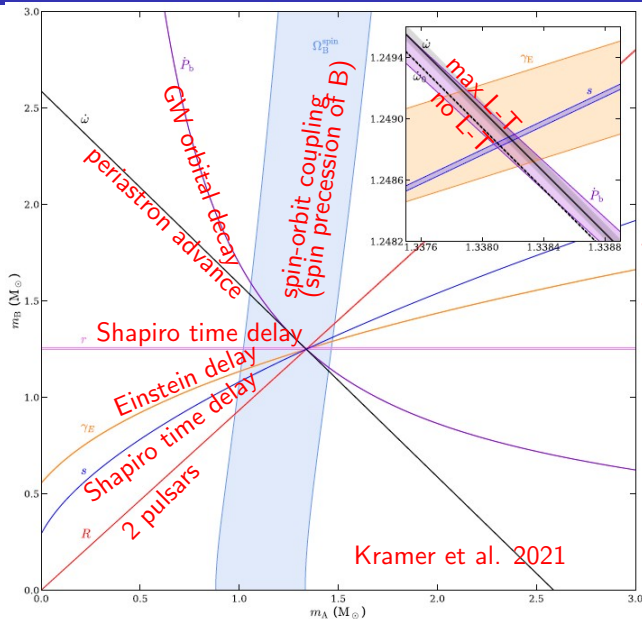
Measurement - Model = Timing Residuals



200ns RMS
over 2 yrs

(From Jacoby et al. 2005, ApJL, 629, 113)

Pulsar Timing for PSR J0737-3039



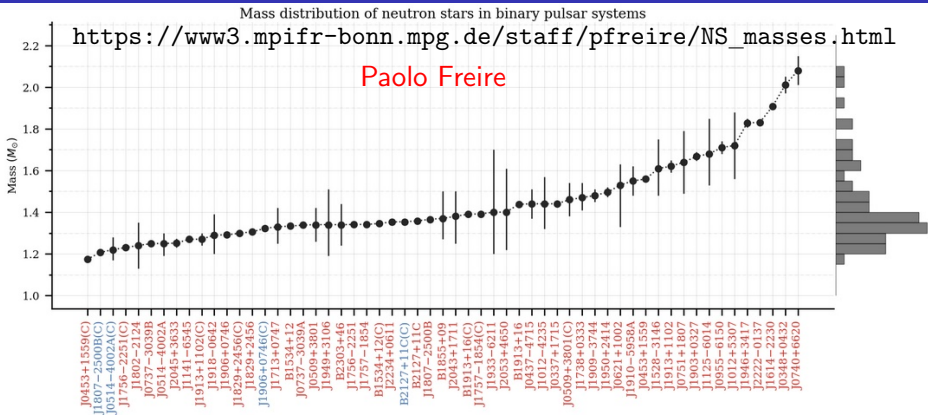
$$m_A = 1.338185_{-14}^{+12} M_\odot$$

$$m_B = 1.248868_{-11}^{+13} M_\odot$$

These are the most precisely known masses of any astronomical object.

Kramer et al. 2021

Masses of Pulsars in Binaries from Pulsar Timing



Largest: $2.08 \pm 0.07 M_{\odot}$

Smallest: $1.174 \pm 0.004 M_{\odot}$

Several other NS masses have been measured by other means, including some of more than $2M_{\odot}$ (e.g., black widow pulsars), but their mass uncertainties are generally large.

How Can a Neutron Star's Radius Be Measured?

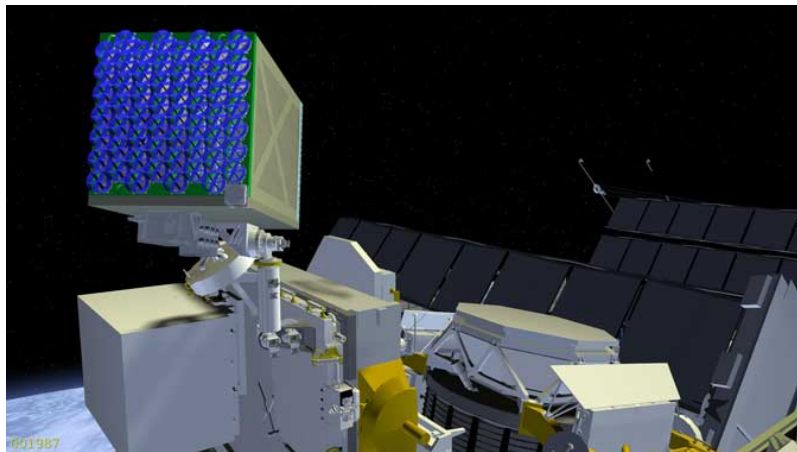
- $\text{Flux} = \frac{\text{Luminosity}}{4\pi D^2} = \frac{4\pi R^2 \sigma_B T_s^4}{4\pi D^2} = \left(\frac{R}{D}\right)^2 \sigma_B T_s^4$
X-ray observations of quiescent neutron stars in low-mass X-ray binaries to measure distance D , Flux and surface temperature T_s . GR effects introduce an R dependence.
- $F_{\text{Edd}} = \frac{GMc}{\kappa D^2}$ X-ray observations of bursting neutron stars in accreting systems to measure the Eddington flux F_{Edd} . κ is the poorly-known opacity. GR effects introduce an R dependence.
- Phase-resolved spectroscopy of millisecond pulsars with nonuniform surface emissions. NICER: PSR J0030+0451, PSR J0437-4715 (closest and brightest millisecond pulsar) and PSR J0740+6620 (most massive pulsar).
- $R_{1.4} = (11.5 \pm 0.3) \frac{\mathcal{M}}{M_\odot} \left(\frac{\tilde{\Lambda}}{800}\right)^{1/6} \text{ km}, \quad \mathcal{M} = \frac{(M_A M_B)^{3/5}}{(M_A + M_B)^{1/5}}$
GW observations of neutron star mergers to measure the chirp mass \mathcal{M} and the binary tidal deformability $\tilde{\Lambda}$ (GW170817).
- $I \propto M_A R_A^2$ Radio observations of spin-orbit coupling in extremely relativistic binary pulsars to measure masses M_A, M_B and moment of inertia I_A [PSR J0737-3039 ($P_b = 0.102\text{d}$), PSR J1757-1854 (0.164 d), PSR J1946+2052 (0.078 d)].

Neutron Star Interior Composition ExploreR (NICER)

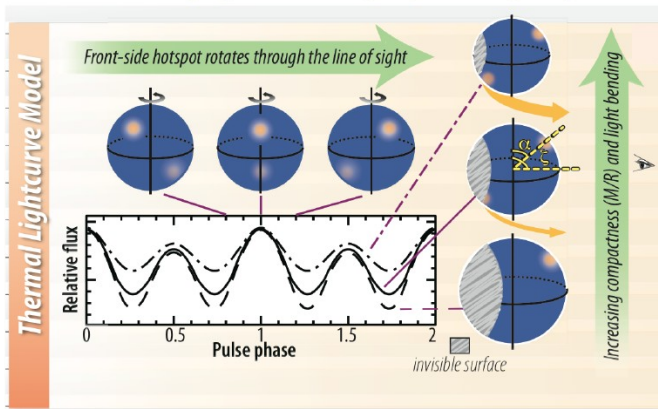
Launched aboard a SpaceX Falcon 9 rocket on June 3, 2017.

It is installed aboard the International Space Station.

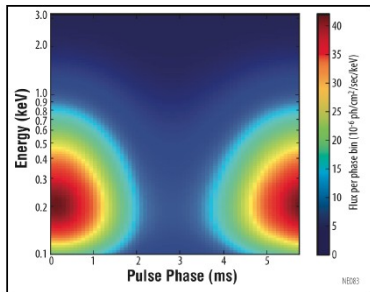
Dedicated to the study of neutron stars through soft X-ray timing.



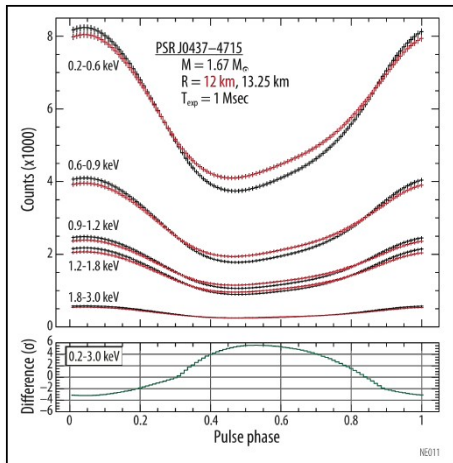
Reveal stellar structure through lightcurve modeling, long-term timing, and pulsation searches



Lightcurve modeling constrains the compactness (M/R) and viewing geometry of a non-accreting millisecond pulsar through the depth of modulation and harmonic content of emission from rotating hot-spots, thanks to **gravitational light-bending**...

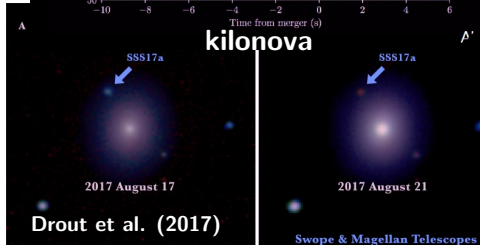
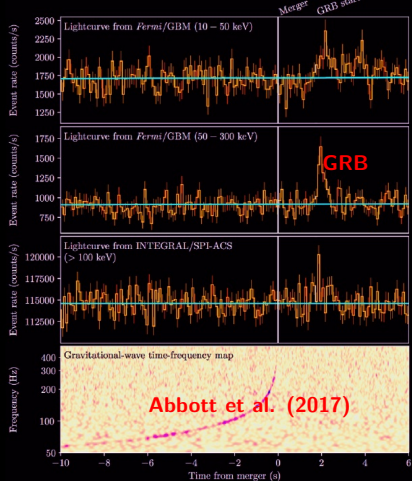


... while phase-resolved spectroscopy promises a direct constraint of radius R .

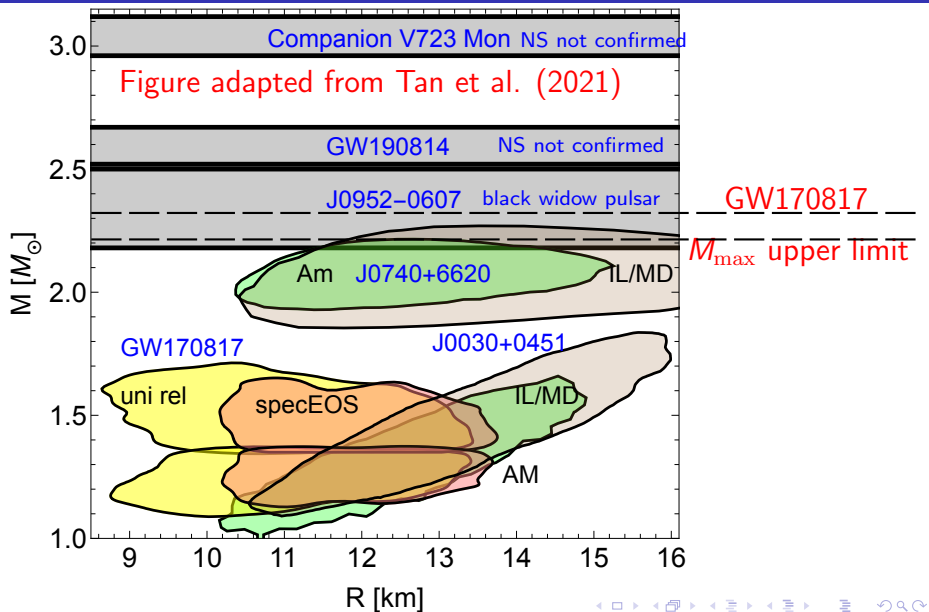


GW170817

- LVC detected a signal consistent with a BNS merger, followed 1.7 s later by a weak gamma-ray burst.
- ~ 10100 orbits observed over 317 s.
- $\mathcal{M} = 1.186 \pm 0.001 M_{\odot}$
- $M_T = M_A + M_B \gtrsim 2^{6/5} \mathcal{M} = 2.725 M_{\odot}$
- $E_{\text{GW}} > 0.025 M_{\odot} c^2$
- $D_L = 40^{+8}_{-14}$ Mpc
- $75 < \tilde{\Lambda} < 560$ ($10.9 \text{ km} < \bar{R} < 13.3 \text{ km}$)
- $M_{\text{ejecta}} \sim 0.06 \pm 0.02 M_{\odot}$
- Blue ejecta: $\sim 0.01 M_{\odot}$
- Red ejecta: $\sim 0.05 M_{\odot}$
- Highly opaque ejecta implies substantial r-process production
- $M_T + \text{Ejecta} + \text{GRB}: M_{\text{max}} \lesssim 2.22 M_{\odot}$



Summary of Astrophysical Observations

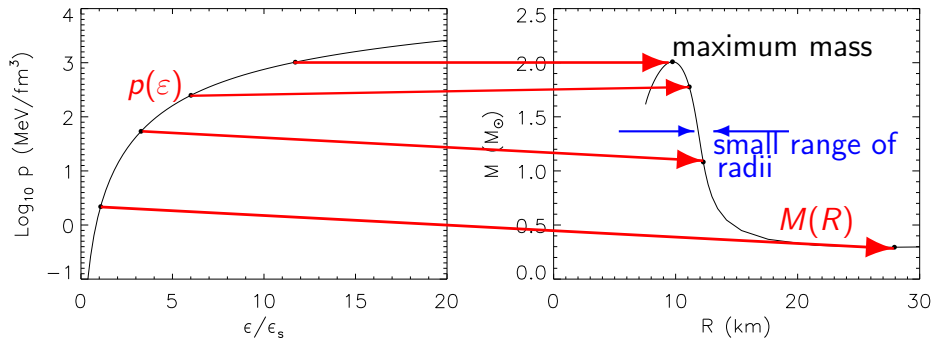


Neutron Star Structure

Tolman-Oppenheimer-Volkov equations

$$\frac{dp}{dr} = -\frac{G}{c^4} \frac{(mc^2 + 4\pi pr^3)(\epsilon + p)}{r(r - 2Gm/c^2)}$$

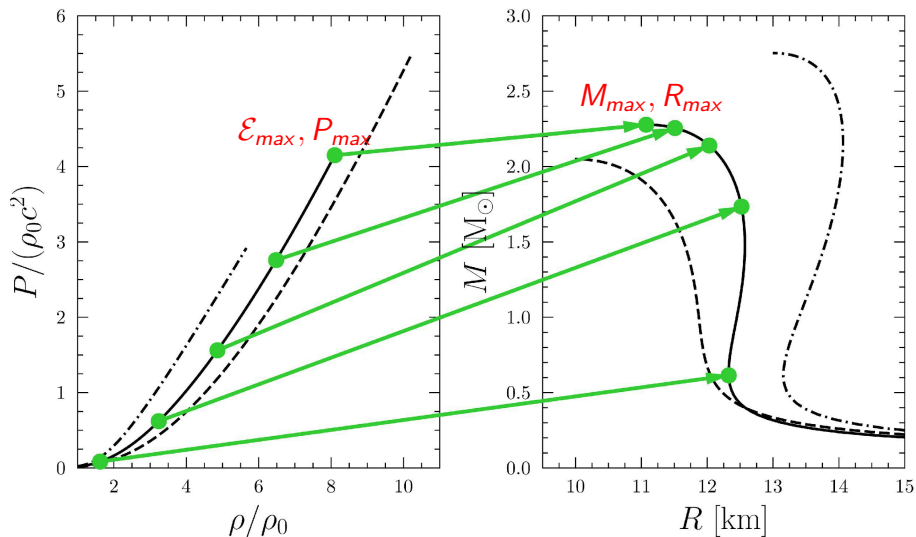
$$\frac{dm}{dr} = 4\pi \frac{\epsilon}{c^2} r^2$$



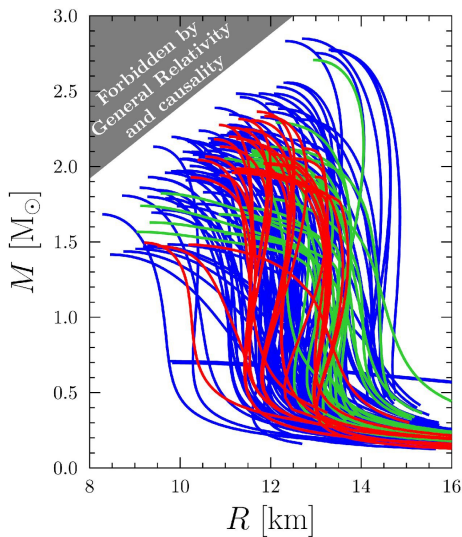
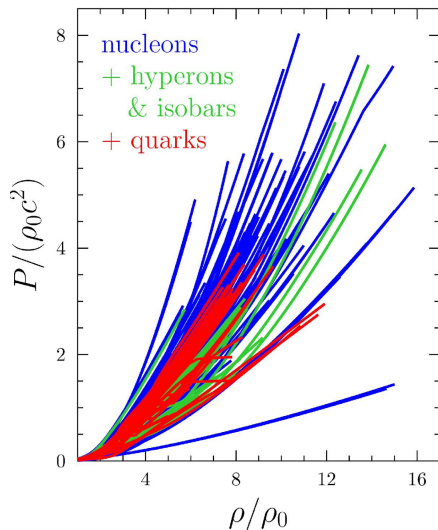
Equation of State

Observations

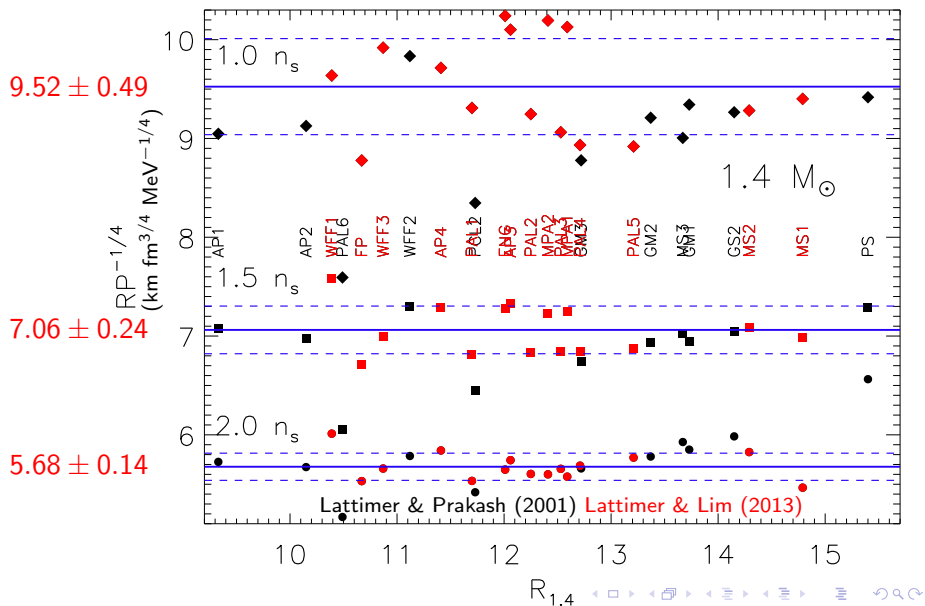
Varying the EOS



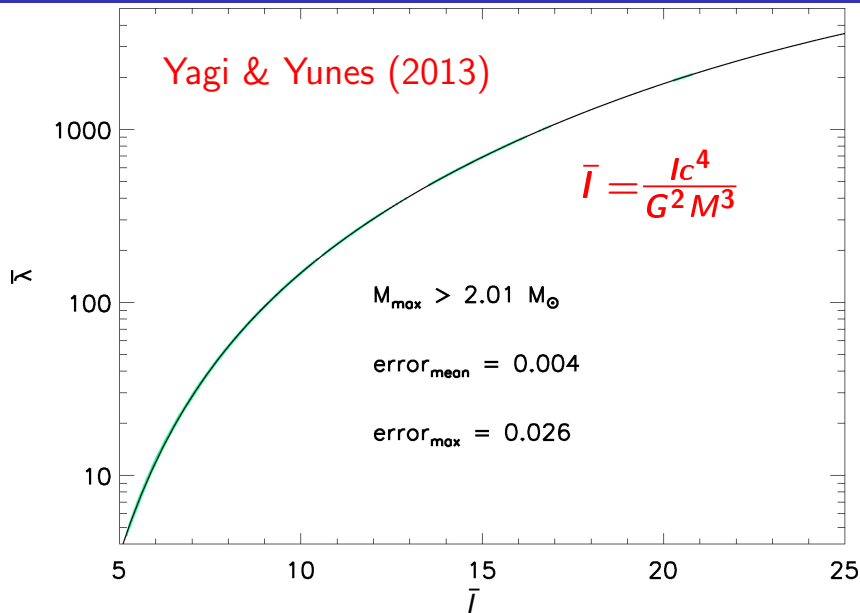
Varying the EOS



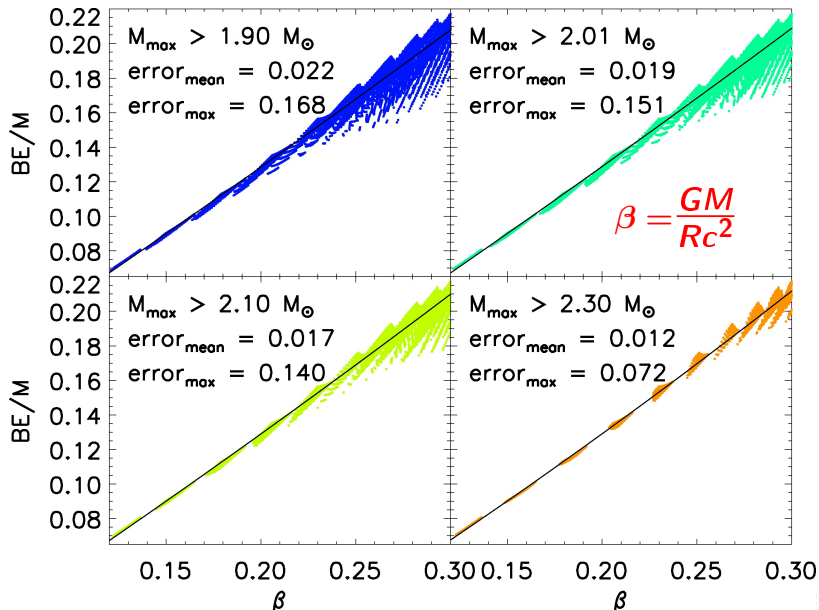
The Radius – Pressure Correlation



Tidal Deformatibility - Moment of Inertia



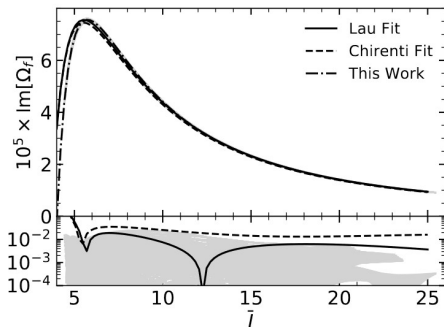
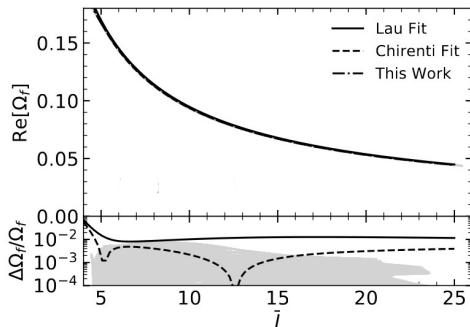
Binding Energy - Compactness



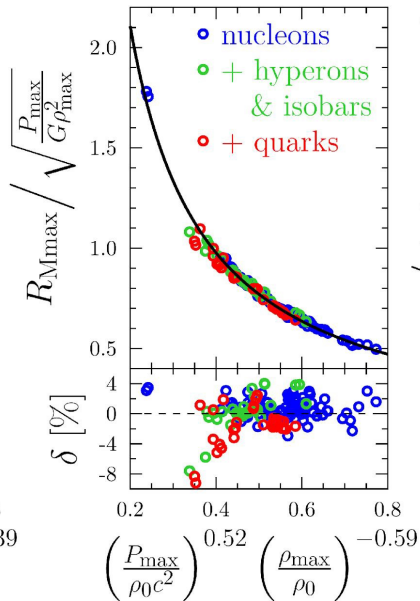
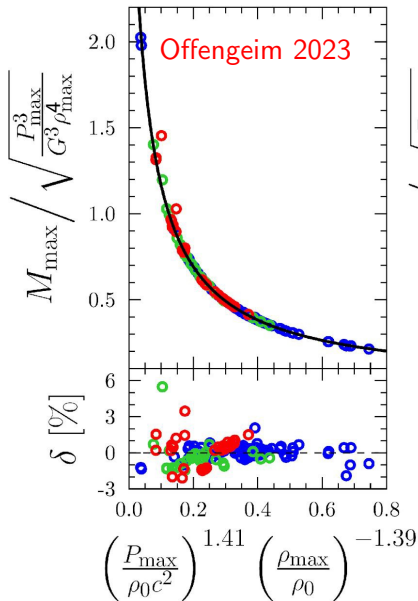
F-Mode Properties - Moment of Inertia

$$\Omega_f = \frac{GM\omega_f}{c^3}$$

Zhao & Lattimer 2022



$M_{\max}, R_{\max}, \mathcal{E}_{\max}, P_{\max}$ Correlation



$M_{\max}, R_{\max}, \mathcal{E}_{\max}, P_{\max}$ Correlation

Offengeim's finding suggest the power-law relations

$$\mathcal{E}_{\max} = (1.809 \pm 0.36) \left(\frac{R_{\max}}{10\text{km}} \right)^{-1.98} \left(\frac{M_{\max}}{M_{\odot}} \right)^{-0.171} \text{GeV fm}^{-3},$$

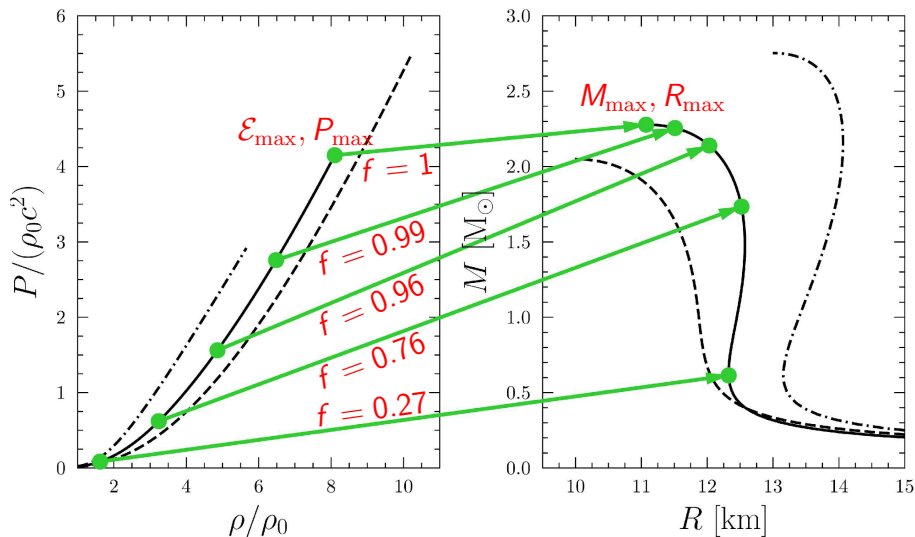
$$P_{\max} = (118.5 \pm 6.2) \left(\frac{R_{\max}}{10\text{km}} \right)^{-5.24} \left(\frac{M_{\max}}{M_{\odot}} \right)^{2.73} \text{MeV fm}^{-3},$$

We found, in addition, that additional points along the $M - R$ curve, at $M = fM_{\max}$, have similarly accurate correlations:

$$\mathcal{E}_f = a_{\mathcal{E},f} \left(\frac{R_{fM_{\max}}}{10\text{km}} \right)^{b_{\mathcal{E},f}} \left(\frac{M_{\max}}{M_{\odot}} \right)^{c_{\mathcal{E},f}},$$

$$P_f = a_{P,f} \left(\frac{R_{fM_{\max}}}{10\text{km}} \right)^{b_{P,f}} \left(\frac{M_{\max}}{M_{\odot}} \right)^{c_{P,f}},$$

Correlations at $M = fM_{\text{max}}$



Correlations With fM_{\max} and 2 R Values

$$\mathcal{E}_f = a_{\mathcal{E},f} \left(\frac{R_{M_1}}{10\text{km}} \right)^{b_{\mathcal{E},f}} \left(\frac{R_{M_2}}{10\text{km}} \right)^{c_{\mathcal{E},f}} \left(\frac{M_{\max}}{M_{\odot}} \right)^d,$$

$$P_f = a_{P,f} \left(\frac{R_{M_1}}{10\text{km}} \right)^{b_{P,f}} \left(\frac{R_{M_2}}{10\text{km}} \right)^{c_{P,f}} \left(\frac{M_{\max}}{M_{\odot}} \right)^{d_{P,f}},$$

$f = M/M_{\max}$	M_1/M_{\max}	M_2/M_{\max}	$\Delta(\ln \mathcal{E}_f)$
1	1	1/2	0.0046047928
4/5	2/3	1/2	0.0035713650
2/3	2/3	3/5	0.0050640415
3/5	4/5	1/2	0.0024633916
1/2	2/3	1/2	0.0047856724
2/5	3/5	1/2	0.0047133738
$f = M/M_{\max}$	M_1/M_{\max}	M_2/M_{\max}	$\Delta(\ln P_f)$
1	1	1/2	0.019032030
4/5	4/5	1/2	0.0096117432
2/3	2/3	3/5	0.014041491
3/5	2/3	1/2	0.00068963633
1/2	3/5	1/2	0.020100887
2/5	3/5	1/2	0.032359011

greatly reduced uncertainties!

Applications

- An analytic method of directly inverting the TOV equations, accuracy can be made arbitrarily high (number of f and R values). Existing techniques use parameterized EOS models in probabilistic (Bayesian) approaches having unquantified systematic uncertainties stemming from the model choice and parameter ranges (prior distributions).
- Correlations of $c_{s,\max}(M_{\max}, R_{\max})$ also exist (Offengeim 2023 found $\sim 10\%$ uncertainty), but accuracies can be improved using ≥ 2 R values. Accurate values for specific f values would be useful for interpolating within the $\mathcal{E} - P$ grid. They could also allow probing the composition of the neutron star interior (phase transitions, etc.).
- Correlations of $\tilde{\Lambda}$, \bar{I} and BE/M with M_{\max} and R_{\max} remain to be explored.